Relative particle yield fluctuations in Pb-Pb collisions at √sNN=2.76 TeV

(ALICE Collaboration) Acharya, S.; ...; Antičić, Tome; ...; Erhardt, Filip; ...; Gotovac, Sven; ...; Jerčić, Marko; ...; ...

THE EUROPEAN
PHYSICAL JOURNAL C

Relative particle yield fluctuations in Pb–Pb collisions at $\sqrt{s_{\mathrm{NN}}} = 2.76$ TeV

ALICE Collaboration[⋆]

CERN, 1211 Geneva 23, Switzerland

Abstract First results on K/π, p/π and K/p fluctuations are obtained with the ALICE detector at the CERN LHC as a function of centrality in Pb–Pb collisions at $\sqrt{s_{\mathrm{NN}}} = 2.76$ TeV. The observable ν_{dyn}, which is defined in terms of the moments of particle multiplicity distributions, is used to quantify the magnitude of dynamical fluctuations of relative particle yields and also provides insight into the correlation between particle pairs. This study is based on a novel experimental technique, called the Identity Method, which allows one to measure the moments of multiplicity distributions in case of incomplete particle identification. The results for p/π show a change of sign in ν_{dyn} from positive to negative towards more peripheral collisions. For central collisions, the results follow the smooth trend of the data at lower energies and ν_{dyn} exhibits a change in sign for p/π and K/p.

1 Introduction

The theory of strong interactions, Quantum Chromodynamics (QCD), predicts that at sufficiently high energy density nuclear matter transforms into a deconfined state of quarks and gluons known as Quark–Gluon Plasma (QGP) [1,2]. One of the possible signatures of a transition between the hadronic and partonic phases is the enhancement of fluctuations of the number of produced particles in the hadronic final state of relativistic heavy-ion collisions [3–5]. Event-by-event fluctuations and correlations may show critical behaviour near the phase boundary, including the crossover region where there is no thermal singularity, in a strict sense, associated with the transition from a QGP phase to a hadron-gas phase. A correlation analysis of event-by-event abundances of pions, kaons and protons produced in Pb–Pb collisions at LHC energies may provide a connection to fluctuations of globally conserved quantities such as electric charge, strangeness and

baryon number, and therefore shed light on the phase structure of strongly interacting matter [6].

In view of the predicted criticality signals at crossover for vanishing net-baryon densities [7], event-by-event fluctuations of relative particle yields are studied using the fluctuation measure $\nu_{\mathrm{dyn}}[A, B]$ [8] defined in terms of moments of particle multiplicity distributions as

$$
\nu_{\mathrm{dyn}}[A, B] = \frac{\langle N_A(N_A - 1)\rangle}{\langle N_A\rangle^2} + \frac{\langle N_B(N_B - 1)\rangle}{\langle N_B\rangle^2} \\ - 2\frac{\langle N_A N_B\rangle}{\langle N_A\rangle\langle N_B\rangle},
\tag{1}
$$

where N_A and N_B are the multiplicities of particles A and B measured event-by-event in a given kinematic range. The $\nu_{\mathrm{dyn}}[A, B]$[1] fluctuation measure contrasts the relative strength of fluctuations of species A and B to the relative strength of correlations between these two species. It vanishes when the particles A and B are produced in a statistically independent way [8,9].

This study at LHC energies is of particular importance for establishing the energy and system size dependence of ν_{dyn} in order to understand the trend observed at lower collision energies from the RHIC Beam Energy Scan (BES) results reported by the STAR collaboration [10]. Furthermore, the advantage of this fluctuation measurement is its robustness against non-dynamical contributions such as those stemming from participant nucleon fluctuations and finite particle detection efficiencies [8,11]. Measurements of the ν_{dyn} observable for net-charge fluctuations were already published by ALICE [12]. Moreover, for identified particles, it was measured at the Super Proton Synchrotron (SPS) [13] and at the Relativistic Heavy-Ion Collider (RHIC) [10] in Pb–Pb and Au–Au collisions, respectively. The ALICE detector at the LHC is ideally suited to extend these measurements to higher collision energies. In particular, the excellent charged-particle tracking and parti-

---

[1] In this study, $\nu_{\mathrm{dyn}}[A, B]$ was taken to be $\nu_{\mathrm{dyn}}[A + \overline{A}, B + \overline{B}]$, where $\overline{A}$ and $\overline{B}$ are the anti-particles of A and B, respectively.

cle identification (PID) capabilities in the central barrel of the detector allow for a precise and differential event-by-event analysis at midrapidity and low transverse momentum (p_T).

The paper is organized as follows. In Sect. 2, details about the ALICE detector setup and the dataset are given. Section 3 discusses the event and track selection criteria, particle identification procedure, and the analysis method. Estimates of statistical and systematic uncertainties are given in Sect. 4. Results on $\nu_{\mathrm{dyn}}[\pi, K]$, $\nu_{\mathrm{dyn}}[\pi, p]$ and $\nu_{\mathrm{dyn}}[p, K]$ in Pb–Pb collisions at $\sqrt{s_{\mathrm{NN}}} = 2.76$ TeV are presented in Sect. 5, and finally Sect. 6 summarizes the measurements presented in this paper.

2 Experimental setup and dataset

ALICE is a general-purpose detector system designed, in particular, for the study of collisions of heavy ions at the LHC. The design, components, and performance of the ALICE detector have been reported elsewhere [14,15]. The ALICE detector is comprised of several detector components organized into a central barrel detection system and forward/backward detectors. The main tracking and PID devices in the central barrel of the experiment are the Inner Tracking System (ITS) and the Time Projection Chamber (TPC), which are operated inside a large solenoidal magnet with $B = 0.5$ T. Two forward scintillator arrays V0-A and V0-C are located on either side of the interaction point and cover the pseudorapidity (η) intervals $2.8 < \eta < 5.1$ and $-3.7 < \eta < -1.7$. The V0 detectors and the two neutron Zero Degree Calorimeters (ZDC), placed at ± 114 m from the interaction point, were used for triggering and event selection.

The ITS-TPC tracking system covers the midrapidity region and provides charged-particle tracking and momentum reconstruction down to $p_T = 100$ MeV/c. The ITS is employed to reconstruct the collision vertex with high precision and to reject charged particles produced in secondary vertices.

The analysis presented in this paper is based on about 13 million minimum-bias Pb–Pb collisions at $\sqrt{s_{\mathrm{NN}}} = 2.76$ TeV collected in the year 2010. The minimum-bias trigger condition is defined by the coincidence of hits in both V0 detectors. In the offline event selection, V0 and ZDC timing information is used to reject beam-gas background and parasitic beam-beam interactions. The definition of the collision centrality is based on the charged-particle multiplicity measured in the V0 detectors [14], which can be related to collision geometry and the number of participating nucleons through a Monte-Carlo (MC) simulation based on a Glauber model [16].

3 Data analysis

3.1 Event and track selection

Charged particles reconstructed in the TPC with full azimuthal acceptance and in the pseudorapidity range of $|\eta| < 0.8$ were used in this analysis. The momentum range was restricted to $0.2 < p < 1.5$ GeV/c in order to minimize systematic uncertainties arising from the overlap of the dE/dx distributions. Furthermore, the following track selection criteria were applied to guarantee optimal dE/dx and momentum resolution, which are crucial for precise particle identification. Charged-particle tracks were accepted in this analysis when they have at least 80 out of a maximum of 159 reconstructed space points in the TPC, and the χ^2 per space point from the track fit is less than 4. Daughter tracks from reconstructed secondary weak-decay kink topologies were rejected. Additional suppression of secondary particles was achieved by restricting the distance-of-closest-approach (DCA) of the extrapolated trajectory to the primary vertex position to less than 2 cm along the beam direction. In the transverse plane the restriction in the DCA depends on p_T in order to take into account the p_T dependence of the impact parameter resolution [17]. The remaining contamination after the DCA cuts is typically less than 10% for the momentum range covered in this work [18].

3.2 Identity method

The standard approach of finding the moments $\langle N_A \rangle$, $\langle N_B \rangle$, $\langle N_A(N_A - 1) \rangle$ and $\langle N_B(N_B - 1) \rangle$ is to count the number of particles N_A and N_B event-by-event and calculate averages over the dataset. However, this approach suffers from incomplete particle identification due to overlapping dE/dx distribution functions, which could be circumvented by either selecting suitable phase-space regions or by using additional detector information such as time-of-flight measurements. These procedures reduce the overall phase-space coverage and detection efficiencies. The present study is based on the Identity Method [19–21] which overcomes the misidentification problem.

The Identity Method was proposed in Ref. [19] as a solution to the misidentification problem for the analysis of events with two different particle species. In Ref. [20], the method was developed further to calculate the second moments of the multiplicity distributions of more than two particle species. Subsequently, in Ref. [21], it was generalized to the first and higher moments of the multiplicity distributions for an arbitrary number of particle species. The first experimental results using the Identity Method were published by the NA49 collaboration [13].

Instead of counting every detected particle event-by-event, the Identity Method follows a probabilistic approach using

Fig. 1 Distributions of ω and W for pions (top), kaons (middle) and protons (bottom) in the momentum interval of $0.3 < p < 0.8$ GeV/c for 0–5% central Pb–Pb events
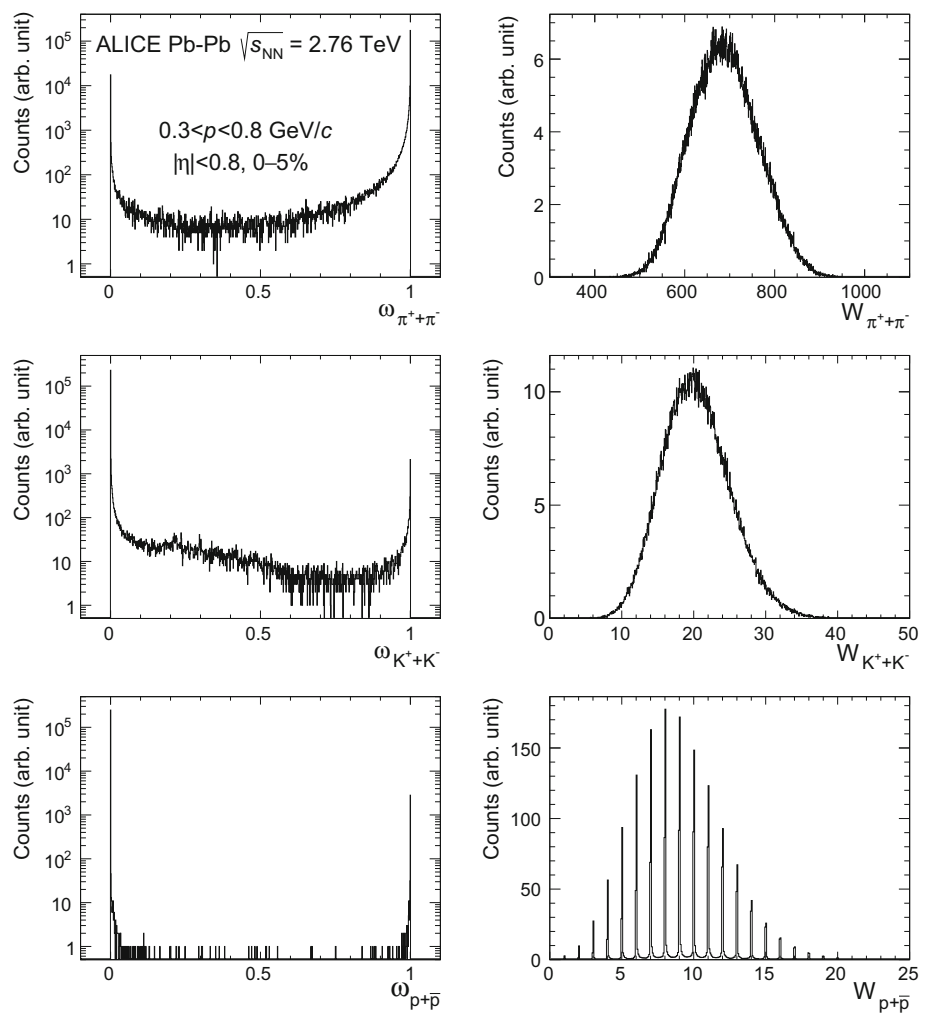
two basic experimental per-track and per-event observables, ω and W, respectively. They are defined as

$$\omega_j(x_i) = \frac{\rho_j(x_i)}{\rho(x_i)} \in [0, 1],$$

$$\rho(x_i) = \sum_j \rho_j(x_i), \quad W_j \equiv \sum_{i=1}^{N(n)} \omega_j(x_i), \qquad (2)$$

where x_i stands for the dE/dx of a given track i, $\rho_j(x)$ is the dE/dx distribution of particle species j within a given phase-space bin and $N(n)$ is the number of tracks in the nth event. The quantity $\omega_j(x_i)$ represents the probability that particle i is of type j. Thus, in case of perfect particle identification, one expects $W_j = N_j$, while this does not hold in case of overlapping dE/dx distributions. Figure 1 shows the ω and W distributions for pions, kaons and protons in the momentum interval of $0.3 < p < 0.8$ GeV/c. The W distribution of protons shows a discrete structure because proton dE/dx distributions have the least overlap.

The moments of the W distributions can be constructed directly from experimental data. The Identity Method calculates the moments of the particle multiplicity distributions

by unfolding the moments of the W distributions with the following matrix operation

$$\langle \overrightarrow{N} \rangle = A^{-1} \langle \overrightarrow{W} \rangle, \qquad (3)$$

where $\langle \overrightarrow{W} \rangle$ and $\langle \overrightarrow{N} \rangle$ are the vectors of the moments of W quantities and unknown true multiplicity distributions, respectively. The response matrix A is defined by the ω quantities. A detailed description of the technique and a demonstration of its robustness can be found in Refs. [20,21].

The dE/dx measurements used as the only input for the Identity Method are obtained from the TPC, which provides a momentum resolution of better than 2% and a single-particle detection efficiency of up to 80% for the kinematic range considered in this paper [14]. The Identity Method employs fits of inclusive dE/dx distributions for the calculation of the ω probabilities entering Eq. 3. Since the overlap regions in the dE/dx distributions are also properly taken into account, a very good description of the inclusive dE/dx spectra, and therefore an excellent understanding of the TPC detector response, is required over the full momentum range covered in this analysis. To this end, the dE/dx distributions
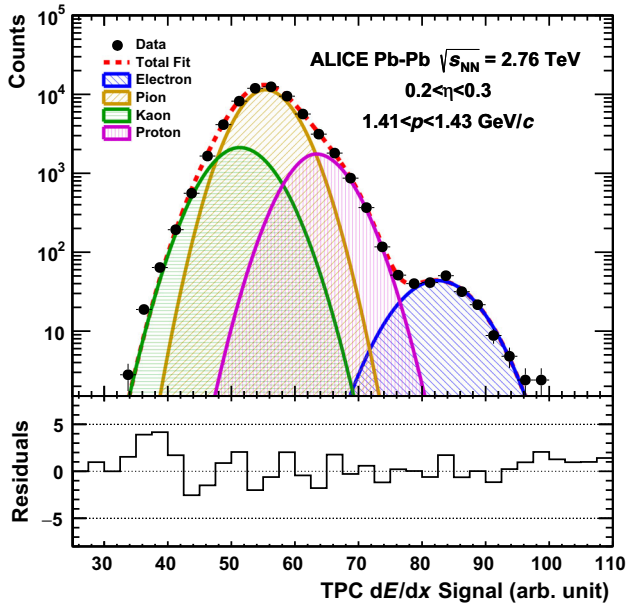
Fig. 2 Distributions of the TPC dE/dx signal of pions, kaons, electrons and protons fitted with the generalized Gaussian function in a given phase-space bin. The residuals are defined as the difference between data points and the total fit function normalized to the statistical error of the data points

of pre-selected samples of pions, protons and electrons, identified by the reconstruction of K_S^0 and Λ decays and photon conversions, were fitted with a generalized Gaussian function of the form:

$$f(x) = Ae^{-(|x-\mu|/\sigma)^\beta}\left(1 + \mathrm{erf}\left(\alpha\frac{|x-\mu|}{\sigma\sqrt{2}}\right)\right) \qquad (4)$$

where A, μ, σ, α and β stand for the abundance, mean, width, skewness and kurtosis of the distribution, respectively. The detector response functions obtained in this way were used later to fit the inclusive dE/dx spectra. To cope with the dependencies of the dE/dx on the track angle and particle multiplicity, fits were performed over the entire pseudorapidity range of $|\eta| < 0.8$ in steps of 0.1 units for each centrality class. Moreover, the momentum intervals were chosen narrow enough to minimize the effect of the momentum dependence on dE/dx, most particularly at low momenta where the magnitude of dE/dx varies rapidly with the momentum. An example of a dE/dx distribution in a given phase-space bin and the corresponding fits are shown in Fig. 2.

4 Statistical and systematic uncertainties

The statistical uncertainties were determined by the number of events in this analysis and the finite number of tracks in each event. The number of events also affects the uncertainty of the shape of the inclusive dE/dx spectra, which is deter-

mined by a fit. This uncertainty enters the calculation of ω and W, and finally the computation of the moments of multiplicity distributions with the Identity Method. Since standard error propagation is impractical given the rather complicated numerical derivation of the final result, the subsample method was chosen to evaluate the statistical uncertainties. To this end, the data set was subdivided into $n = 25$ random subsamples i. The ν_{dyn} values were reconstructed for each subsample and the statistical uncertainty was obtained according to

$$\sigma_{\langle \nu_{\mathrm{dyn}}\rangle} = \frac{\sigma}{\sqrt{n}}, \qquad (5)$$

where

$$\sigma = \sqrt{\frac{\sum_i(\nu_{\mathrm{dyn},i} - \langle \nu_{\mathrm{dyn}}\rangle)^2}{n-1}}, \quad \langle \nu_{\mathrm{dyn}}\rangle = \frac{1}{n}\sum_i \nu_{\mathrm{dyn},i}. \qquad (6)$$

The summary of all sources of systematic uncertainties is shown in Table 1 and in the next paragraphs the main contributors to the systematics are detailed.

The largest contribution to the total systematic uncertainty is from the fits of the measured particle dE/dx distributions. The quality of the fits was monitored by Kolmogorov–Smirnov (K–S) and χ^2 tests. To study the influence of possible systematic shifts in the fit parameters on ν_{dyn}, the fit parameters of each particle in the overlap regions were varied by about $\pm 0.5\%$, which defines the boundaries where the K–S test fails at 90% confidence level. The observed maximum variations range from about 7% to 15% for $\nu_{\mathrm{dyn}}[\pi, \mathrm{p}]$ and $\nu_{\mathrm{dyn}}[\pi, \mathrm{K}]$, respectively.

Even though ν_{dyn} is known to be robust against detection-efficiency losses, it may show an explicit dependence if the detector response functions differ from Binomial or the efficiencies exhibit large variations with detector occupancy [8]. Therefore, one also has to investigate the uncertainty resulting from the detection efficiency losses. For that, the ν_{dyn} results reconstructed from a full Monte Carlo simulation of HIJING [22,23] events employing a GEANT3 [24] implementation of the ALICE detector were compared to the analysis at the generator level, where in both generated and reconstructed levels perfect PID information was used. The resulting systematic uncertainty from the finite tracking efficiency is less than 6%.

The systematic uncertainties due to the track selection criteria were estimated by a variation of the selection ranges. The systematics from contamination of weak decays and other secondary particles were obtained by varying the DCA cuts. Other contributions to the total systematic uncertainty arise from the cuts applied on the maximum distance of the reconstructed vertex to the nominal interaction point along the beam axis, the number of required TPC space points per

Table 1 List of contributions to the systematic uncertainty of the particle ratio fluctuations

Uncertainty source	$\nu_{dyn}[\pi, K]$ (%)	$\nu_{dyn}[\pi, p]$ (%)	$\nu_{dyn}[p, K]$ (%)
Inclusive dE/dx fits	10–15	4–7	8–12
Detection efficiency	0.5–6	0.5–4	0.5–5
DCA to vertex	1–4	1–2	1–3
Vertex z position	0.5–2	0.5–1	0.5–2
TPC $\chi^2/d.o.f.$	1–3	1–2	1–3
Min. TPC space points	0.5–3	0.5–2	0.5–3
B-field polarity	0.5–2	0.5–1	0.5–2
Total systematic uncertainty	10–17	4–9	8–14

Table 2 Numerical values of ν_{dyn} results for different particle pairs. The first uncertainty is statistical and the second systematic

Centrality (%)	$\langle dN_{ch}/d\eta \rangle$	$\nu_{dyn}[\pi, K]$ (10^{-3})	$\nu_{dyn}[\pi, p]$ (10^{-3})	$\nu_{dyn}[p, K]$ (10^{-3})
0–5	1601 ± 60	$1.35 \pm 0.08 \pm 0.25$	$0.59 \pm 0.08 \pm 0.13$	$0.59 \pm 0.08 \pm 0.13$
5–10	1294 ± 49	$1.22 \pm 0.08 \pm 0.22$	$0.19 \pm 0.08 \pm 0.06$	$0.46 \pm 0.10 \pm 0.11$
10–20	966 ± 37	$1.35 \pm 0.08 \pm 0.21$	$0.38 \pm 0.08 \pm 0.12$	$0.98 \pm 0.10 \pm 0.17$
20–30	649 ± 23	$1.69 \pm 0.09 \pm 0.21$	$0.29 \pm 0.09 \pm 0.15$	$1.76 \pm 0.13 \pm 0.34$
30–40	426 ± 15	$2.27 \pm 0.11 \pm 0.25$	$0.01 \pm 0.18 \pm 0.18$	$2.39 \pm 0.24 \pm 0.40$
40–50	261 ± 9	$3.52 \pm 0.16 \pm 0.37$	$-0.49 \pm 0.18 \pm 0.22$	$3.64 \pm 0.32 \pm 0.57$
50–60	149 ± 6	$6.43 \pm 0.26 \pm 0.96$	$-1.38 \pm 0.24 \pm 0.29$	$6.54 \pm 0.47 \pm 0.92$
60–70	76 ± 4	$11.91 \pm 0.53 \pm 2.1$	$-4.90 \pm 0.58 \pm 0.56$	$10.34 \pm 1.0 \pm 1.8$
70–80	35 ± 2	$29.99 \pm 1.2 \pm 4.0$	$-16.02 \pm 1.5 \pm 1.1$	$17.93 \pm 2.0 \pm 3.3$

track and the χ^2 per degree of freedom of the track fit. Moreover, the effect of the magnetic field polarity was investigated by separate analyses of data taken under two polarities. Neither of these contributions to the total systematic uncertainty exceeds 5%. The total systematic uncertainty was obtained by adding in quadrature the individual maximum systematic variations from these different contributions.

5 Results

5.1 Centrality dependence and comparison to models

In this section, the results are presented as a function of collision centrality and compared to calculations with the HIJING [22,23] and AMPT [25] models. The unscaled values of ν_{dyn} for different combinations of particles in each centrality class, together with the final statistical and systematic uncertainties, are given in Table 2. Due to the intrinsic multiplicity dependence of ν_{dyn}, discussed in Refs [26,27], the values of ν_{dyn} were scaled further by the charged-particle multiplicity density at midrapidity, $dN_{ch}/d\eta$. The fully corrected experimental $dN_{ch}/d\eta$ values were taken from Ref. [18]. Figure 3 shows measured values of ν_{dyn} scaled by $dN_{ch}/d\eta$ as a function of the collision centrality expressed in terms of $dN_{ch}/d\eta$. The values for ν_{dyn} and $dN_{ch}/d\eta$ for HIJING and AMPT were calculated by using corresponding particle multiplicities at the generator level within the same experimental acceptance.

A flat behaviour is expected in this representation if a superposition of independent particle sources is assumed, as in the Wounded Nucleon Model (WNM) [28].

Measured values of $\nu_{dyn}[\pi, K]$ and $\nu_{dyn}[p, K]$ are positive across the entire centrality range, while $\nu_{dyn}[\pi, p]$ is negative for the most peripheral collisions and changes sign at mid-central collisions. The centrality dependencies observed in $\nu_{dyn}[p, K]$ and $\nu_{dyn}[\pi, p]$ are similar in shape, being flat from central to mid-central collisions and systematically decreasing for the most peripheral ones. In contrast, $\nu_{dyn}[\pi, K]$ is almost independent of centrality from most peripheral to mid-central collisions and rises as the centrality increases. A similar qualitative behaviour is also observed for $\nu_{dyn}[\pi, K]$ within the kinematic range of $|\eta| < 1$ and $0.2 < p < 0.6$ GeV/c as measured in Au–Au collisions at $\sqrt{s_{NN}} = 200$ GeV by the STAR collaboration. The difference in the absolute values is, to a large extent, due to the increase in $dN_{ch}/d\eta$ by almost a factor of two between the two collision energies. The same argument holds true for the most central STAR data at 62.4 GeV, although the centrality dependence is rather flat in this case [27]. The overall behaviour is defined by the interplay between correlation and fluctuation terms encoded in the definition of the ν_{dyn} observable. To disentangle these terms, one needs a dedicated study focusing on separate charge combinations, which also makes it possible to investigate contributions from resonance decays and global charge conservations.
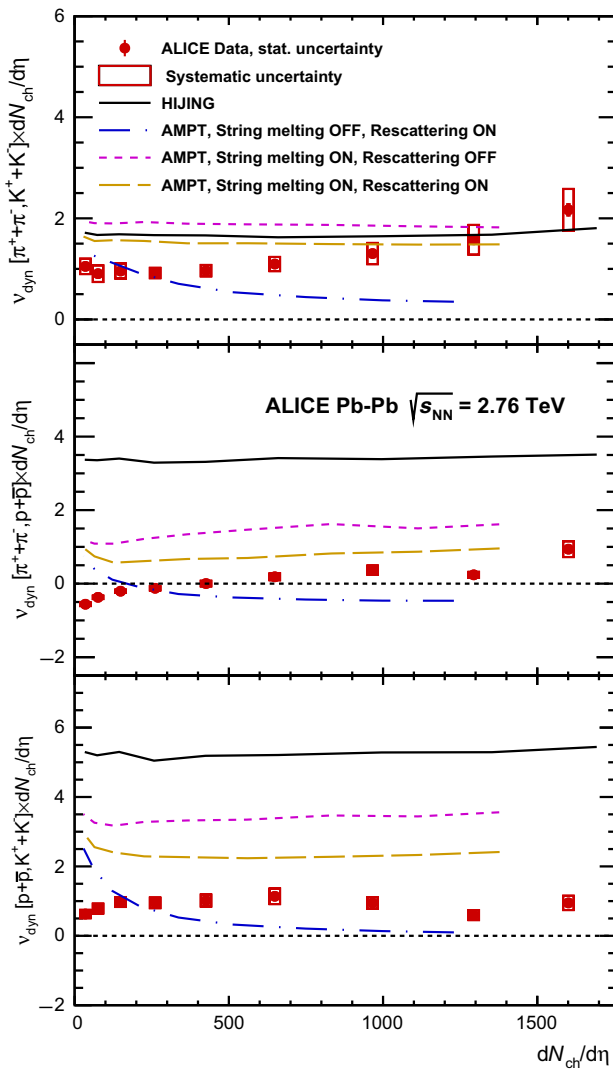
Fig. 3 Results for $\nu_{dyn}[\pi, K]$, $\nu_{dyn}[\pi, p]$ and $\nu_{dyn}[p, K]$ scaled by the charged-particle density $dN_{ch}/d\eta$. The ALICE data are shown by red markers while the coloured lines indicate the HIJING [22,23] and AMPT [25] model calculations. The data are shown as a function of the collision centrality, expressed in terms of $dN_{ch}/d\eta$

An important characteristic of HIJING is that it treats nucleus-nucleus collisions as an independent superposition of nucleon-nucleon interactions. As such, it does not incorporate mechanisms for final-state interactions among the produced particles and therefore phenomena such as equilibrium and collectivity do not occur. The AMPT calculations are performed with three different settings including (1) string melting, (2) hadronic rescattering, and (3) string melting and hadronic rescattering. All three versions of the AMPT model presented here use hard minijet partons and soft strings from HIJING as initial conditions. Partonic evolution is described by Zhang's parton cascade (ZPC) [29] which is followed by a hadronization process. In the last step, hadronic rescattering and the decay of resonances takes place. In the default AMPT

model, after minijet partons stop interacting with other partons, they are combined with their parent strings to form excited strings, which are then converted to hadrons according to the Lund string fragmentation model [25]. However, in the string melting scenario, instead of employing the Lund string fragmentation mechanism, hadronization is modeled via a quark coalescence scheme by combining two nearest quarks into a meson and three nearest quarks (antiquarks) into a baryon (antibaryon). This ultimately reduces the correlation between produced hadrons.

HIJING produces positive values for the three particle pair combinations and does not exhibit any non-monotonic behaviour as a function of centrality, even though it implements exact global conservation laws. In contrast, hadronic rescattering produces additional resonances at the hadronization phase thereby introducing additional correlations between particles [25]. Consequently, the AMPT configuration with hadronic rescattering drives the ν_{dyn} results towards negative values as the collision centrality increases. In particular, for $\nu_{dyn}[\pi, p]$, contrary to the data, it predicts negative values. On the other hand, the AMPT version with string melting shows a weak centrality dependence for the three particle pair combinations. None of the models investigated in this work give a reasonable quantitative description of the measured data.

5.2 Energy dependence

Values of ν_{dyn} measured in this work for the most central Pb–Pb collisions were compared to NA49 and STAR data in Fig. 4. Measurements from NA49 and STAR show a smooth evolution of ν_{dyn} with collision energy and do not reveal any indications for critical behaviour in the range $6.3 < \sqrt{s_{NN}} < 200$ GeV. The apparent differences between NA49 and STAR data for $\nu_{dyn}[p, K]$ and $\nu_{dyn}[\pi, K]$ at $\sqrt{s_{NN}} < 10$ GeV were traced back in Ref. [13] to the dependence of ν_{dyn} on the detector acceptance. Above this energy, both experiments report positive values for $\nu_{dyn}[\pi, K]$, and a weak dependence on the collision energy, whereas $\nu_{dyn}[p, K]$ is negative and approaches zero as the collision energy increases.

ALICE data are positive for the three particle pair combinations and follow the trend observed at lower energies, involving a sign change for $\nu_{dyn}[\pi, p]$ and $\nu_{dyn}[p, K]$ as a function of energy. Such a change of sign has been predicted by transport models HSD [30] and UrQMD [31] in the RHIC energy regime [10]. Since neither HSD nor UrQMD explicitly include the quark and gluon degrees of freedom, this observation can be attributed to the particular realization of the string and resonance dynamics used in the models [30]. Additionally, HIJING and AMPT model calculations at LHC energies predict positive values except for $\nu_{dyn}[\pi, p]$ in the AMPT configuration with hadronic rescattering and without string melting. To understand the difference between the

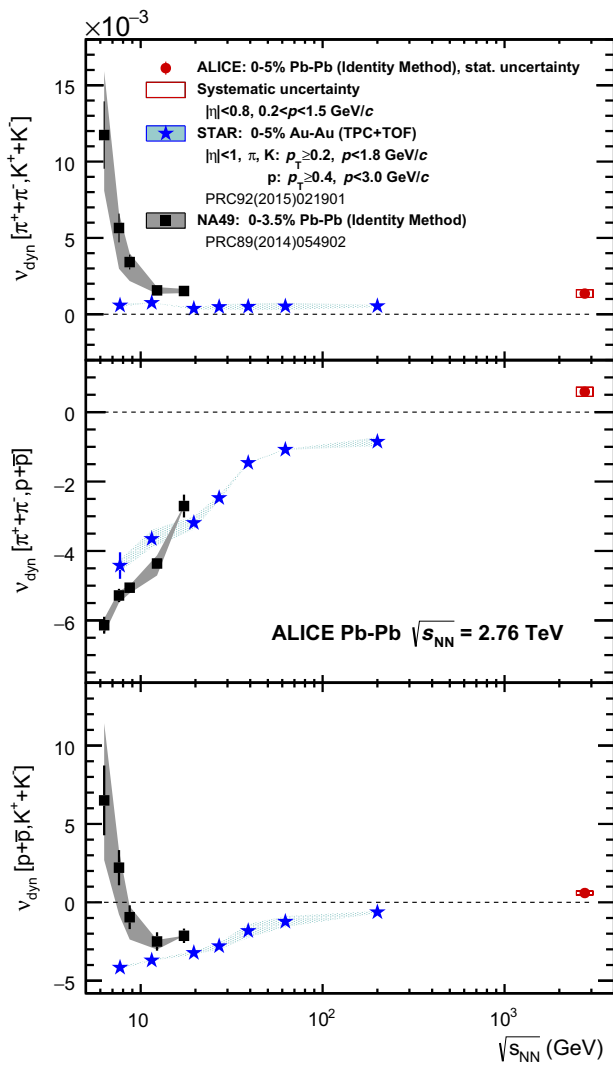**Fig. 4** Collision-energy dependence of ν_{dyn}. Results obtained with the Identity Method in this work and by the NA49 collaboration [13] in Pb–Pb collisions are shown with red circles and black squares, respectively, while those obtained by the STAR collaboration [10] in Au–Au collisions are shown with blue stars

STAR and ALICE results, the acceptance dependence of ν_{dyn} was also investigated with the ALICE data by varying the phase-space coverage. Opening the pseudorapidity window from $|\eta| < 0.8$ up to $|\eta| < 1$ yields a reduction in ν_{dyn} of 10-20%. However, this reduction is insufficient to explain the difference between the ALICE and STAR results, most particularly the sign change with increasing energy.

6 Summary

In summary, measurements of ν_{dyn} in Pb–Pb collisions at $\sqrt{s_{\mathrm{NN}}} = 2.76$ TeV for three specific particle pair combinations using the Identity Method were presented. Values

of ν_{dyn}, scaled by the charged-particle density at midrapidity $dN_{\mathrm{ch}}/d\eta$, exhibit finite variations with collision centrality. This is in contrast to predictions by HIJING, which, for all three pair combinations, show essentially constant as well as positive values. The results for $\nu_{\mathrm{dyn}}[\pi, K]$ and $\nu_{\mathrm{dyn}}[p, K]$ are positive across the entire centrality range, while $\nu_{\mathrm{dyn}}[\pi, p]$ changes sign from positive to negative towards more peripheral collisions suggesting differences in the production dynamics of these pairs. The centrality dependence of $\nu_{\mathrm{dyn}}[\pi, K]$ shows a similar behaviour, increasing with centrality, as measured in Au–Au collisions at $\sqrt{s_{\mathrm{NN}}} = 200$ GeV by the STAR collaboration, while the data at $\sqrt{s_{\mathrm{NN}}} = 62.4$ GeV shows no centrality dependence. Comparisons with calculations from the AMPT model, using three distinct configurations, show that AMPT is unable to reproduce measured data in this work. Calculations with quark coalescence show only a very slight centrality dependence and no sign changes. On the other hand, AMPT values with hadronic rescattering and no quark coalescence decrease significantly with increasing collision centrality and exhibit a sign change towards central collisions in the case of $\nu_{\mathrm{dyn}}[\pi, p]$. The evolution of ν_{dyn} with collision energy shows that the particle production dynamics changes significantly from that observed at lower energies. Values of ν_{dyn} measured with all three pair combinations follow a smooth continuation of the data measured by STAR and exhibit a change in sign for $\nu_{\mathrm{dyn}}[p, K]$ and $\nu_{\mathrm{dyn}}[\pi, p]$. The analysis of ν_{dyn} with enlarged acceptance shows that the magnitude of ν_{dyn} depends on the kinematical limits but the change appears too small to explain the difference with the STAR results. A more detailed analysis of fluctuations with charge and species specific pairs is required to fully characterize the particle production dynamics in heavy-ion collisions and understand, in particular, the origin of the sign changes reported in this work.

References

1. J.C. Collins, M.J. Perry, Superdense matter: neutrons or asymptotically free quarks? Phys. Rev. Lett. **34**, 1353 (1975)
2. E.V. Shuryak, Quantum chromodynamics and the theory of superdense matter. Phys. Rep. **61**, 71–158 (1980)
3. M.A. Stephanov, K. Rajagopal, E.V. Shuryak, Signatures of the tricritical point in QCD. Phys. Rev. Lett. **81**, 4816–4819 (1998). arXiv:hep-ph/9806219 [hep-ph]
4. E.V. Shuryak, M.A. Stephanov, When can long range charge fluctuations serve as a QGP signal? Phys. Rev. C **63**, 064903 (2001). arXiv:hep-ph/0010100 [hep-ph]
5. HotQCD Collaboration, A. Bazavov, et al., Fluctuations and Correlations of net baryon number, electric charge, and strangeness: a comparison of lattice QCD results with the hadron resonance gas model. Phys. Rev. D **86**, 034509 (2012). arXiv:1203.0784 [hep-lat]
6. V. Koch, Hadronic fluctuations and correlations, in R. Stock (ed.), *Relativistic Heavy Ion Physics* (Springer, Heidelberg, 2010), pp. 626–652. http://materials.springer.com/lb/docs/sm_lbs_978-3-642-01539-7_20
7. A. Bazavov et al., The chiral and deconfinement aspects of the QCD transition. Phys. Rev. D **85**, 054503 (2012). arXiv:1111.1710 [hep-lat]
8. C. Pruneau, S. Gavin, S. Voloshin, Methods for the study of particle production fluctuations. Phys. Rev. C **66**, 044904 (2002). arXiv:nucl-ex/0204011 [nucl-ex]
9. P. Christiansen, E. Haslum, E. Stenlund, Number-ratio fluctuations in high-energy particle production. Phys. Rev. C **80**, 034903 (2009). arXiv:0902.4788 [hep-ex]
10. STAR Collaboration, N.M. Abdelwahab et al., Energy Dependence of K/π, p/π, and K/p Fluctuations in Au+Au Collisions from $\sqrt{s_{NN}}$ = 7.7 to 200 GeV. Phys. Rev. C **92**(2), 021901 (2015). arXiv:1410.5375 [nucl-ex]
11. P. Braun-Munzinger, A. Rustamov, J. Stachel, Bridging the gap between event-by-event fluctuation measurements and theory predictions in relativistic nuclear collisions. Nucl. Phys. A **960**, 114–130 (2017). arXiv:1612.00702 [nucl-th]
12. ALICE Collaboration, B. Abelev et al., Net-charge fluctuations in Pb–Pb collisions at $\sqrt{s_{NN}}$ = 2.76 TeV. Phys. Rev. Lett. **110**(15), 152301 (2013). arXiv:1207.6068 [nucl-ex]
13. T. Anticic et al., Phase-space dependence of particle-ratio fluctuations in Pb + Pb collisions from 20 A to 158 A GeV beam energy. Phys. Rev. C **89**(5), 054902 (2014). arXiv:1310.3428 [nucl-ex]
14. ALICE Collaboration, B.B. Abelev et al., Performance of the ALICE Experiment at the CERN LHC. Int. J. Mod. Phys. A **29**, 1430044 (2014). arXiv:1402.4476 [nucl-ex]
15. ALICE Collaboration, K. Aamodt et al., The ALICE experiment at the CERN LHC. JINST **3**, S08002 (2008)
16. C. Loizides, J. Nagle, P. Steinberg, Improved version of the PHOBOS Glauber Monte Carlo, SoftwareX (1–2), 13–18 (2015) arXiv:1408.2549 [nucl-ex]. https://doi.org/10.1016/j.softx.2015.05.001
17. ALICE Collaboration, K. Aamodt, et al., Suppression of charged particle production at large transverse momentum in central Pb–Pb collisions at $\sqrt{s_{NN}}$ = 2.76 TeV. Phys. Lett. B **696**, 30–39 (2011). arXiv:1012.1004 [nucl-ex]
18. ALICE Collaboration, B. Abelev, et al., Centrality dependence of π, K, p production in Pb–Pb collisions at $\sqrt{s_{NN}}$ = 2.76 TeV. Phys. Rev. C **88**, 044910 (2013). arXiv:1303.0737 [hep-ex]
19. M. Gazdzicki, K. Grebieszkow, M. Mackowiak, S. Mrowczynski, Identity method to study chemical fluctuations in relativistic heavy-ion collisions. Phys. Rev. C **83**, 054907 (2011). arXiv:1103.2887 [nucl-th]

20. M.I. Gorenstein, Identity method for particle number fluctuations and correlations. Phys. Rev. C **84**, 024902 (2011). arXiv:1106.4473 [nucl-th]

21. A. Rustamov, M.I. Gorenstein, Identity method for moments of multiplicity distribution. Phys. Rev. C **86**, 044906 (2012). arXiv:1204.6632 [nucl-th]

22. M. Gyulassy, X.-N. Wang, HIJING 1.0: a Monte Carlo program for parton and particle production in high-energy hadronic and nuclear collisions. Comput. Phys. Commun. **83**, 307 (1994). arXiv:nucl-th/9502021 [nucl-th]

23. W.-T. Deng, X.-N. Wang, R. Xu, Hadron production in p+p, p+Pb, and Pb+Pb collisions with the HIJING 2.0 model at energies available at the CERN Large Hadron Collider. Phys. Rev. **C83**, 014915 (2011). arXiv:1008.1841 [hep-ph]

24. R. Brun, F. Bruyant, F. Carminati, S. Giani, M. Maire, A. McPherson, G. Patrick, L. Urban, GEANT detector description and simulation tool, CERN-W5013. Tech. rep., CERN (1994). http://cds.cern.ch/record/1082634

25. Z.-W. Lin, C.M. Ko, B.-A. Li, B. Zhang, S. Pal, A multi-phase transport model for relativistic heavy ion collisions. Phys. Rev. C **72**, 064901 (2005). arXiv:nucl-th/0411110 [nucl-th]

26. V. Koch, T. Schuster, On the energy dependence of K/pi fluctuations in relativistic heavy ion collisions. Phys. Rev. C **81**, 034910 (2010). arXiv:0911.1160 [nucl-th]

27. S.T.A.R. Collaboration, B.I. Abelev et al., K/pi fluctuations at relativistic energies. Phys. Rev. Lett. **103**, 092301 (2009). arXiv:0901.1795 [nucl-ex]

28. A. Bialas, M. Bleszynski, W. Czyz, Multiplicity distributions in nucleus–nucleus collisions at high-energies. Nucl. Phys. B **111**, 461–476 (1976)

29. B. Zhang, ZPC 1.0.1: a Parton cascade for ultrarelativistic heavy ion collisions. Comput. Phys. Commun. **109**, 193–206 (1998). arXiv:nucl-th/9709009 [nucl-th]

30. M.I. Gorenstein, M. Hauer, V.P. Konchakovski, E.L. Bratkovskaya, Fluctuations of the K/pi ratio in nucleus–nucleus collisions: statistical and transport models. Phys. Rev. C **79**, 024907 (2009). arXiv:0811.3089 [nucl-th]

31. M. Bleicher et al., Relativistic hadron hadron collisions in the ultra-relativistic quantum molecular dynamics model. J. Phys. G **25**, 1859–1896 (1999). arXiv:hep-ph/9909407 [hep-ph]

ALICE Collaboration

S. Acharya[137], D. Adamová[94], J. Adolfsson[34], M. M. Aggarwal[99], G. Aglieri Rinella[35], M. Agnello[31], N. Agrawal[48], Z. Ahammed[137], S. U. Ahn[79], S. Aiola[141], A. Akindinov[64], M. Al-Turany[106], S. N. Alam[137], D. S. D. Albuquerque[122], D. Aleksandrov[90], B. Alessandro[58], R. Alfaro Molina[74], Y. Ali[15], A. Alici[12,27,53], A. Alkin[3], J. Alme[22], T. Alt[70], L. Altenkamper[22], I. Altsybeev[136], C. Alves Garcia Prado[121], C. Andrei[87], D. Andreou[35], H. A. Andrews[110], A. Andronic[106], V. Anguelov[104], C. Anson[97], T. Antičić[107], F. Antinori[56], P. Antonioli[53], L. Aphecetche[114], H. Appelshäuser[70], S. Arcelli[27], R. Arnaldi[58], O. W. Arnold[36,105], I. C. Arsene[21], M. Arslandok[104], B. Audurier[114], A. Augustinus[35], R. Averbeck[106], M. D. Azmi[17], A. Badalà[55], Y. W. Baek[60,78], S. Bagnasco[58], R. Bailhache[70], R. Bala[101], A. Baldisseri[75], M. Ball[45], R. C. Baral[67,88], A. M. Barbano[26], R. Barbera[28], F. Barile[33], L. Barioglio[26], G. G. Barnaföldi[140], L. S. Barnby[93], V. Barret[131], P. Bartalini[7], K. Barth[35], E. Bartsch[70], N. Bastid[131], S. Basu[139], G. Batigne[114], B. Batyunya[77], P. C. Batzing[21], J. L. BazoAlba[111], I. G. Bearden[91], H. Beck[104], C. Bedda[63], N. K. Behera[60], I. Belikov[133], F. Bellini[27,35], H. Bello Martinez[2], R. Bellwied[124], L. G. E. Beltran[120], V. Belyaev[83], G. Bencedi[140], S. Beole[26], A. Bercuci[87], Y. Berdnikov[96], D. Berenyi[140], R. A. Bertens[127], D. Berzano[35], L. Betev[35], A. Bhasin[101], I. R. Bhat[101], B. Bhattacharjee[44], J. Bhom[118], A. Bianchi[26], L. Bianchi[124], N. Bianchi[51], C. Bianchin[139], J. Bielčík[39], J. Bielčíková[94], A. Bilandzic[36,105], G. Biro[140], R. Biswas[4], S. Biswas[4], J. T. Blair[119], D. Blau[90], C. Blume[70], G. Boca[134], F. Bock[35], A. Bogdanov[83], L. Boldizsár[140], M. Bombara[40], G. Bonomi[135], M. Bonora[35], J. Book[70], H. Borel[75], A. Borissov[19,104], M. Borri[126], E. Botta[26], C. Bourjau[91], L. Bratrud[70], P. Braun-Munzinger[106], M. Bregant[121], T. A. Broker[70], M. Broz[39], E. J. Brucken[46], E. Bruna[58], G. E. Bruno[33,35], D. Budnikov[108], H. Buesching[70], S. Bufalino[31], P. Buhler[113], P. Buncic[35], O. Busch[130], Z. Buthelezi[76], J. B. Butt[15], J. T. Buxton[18], J. Cabala[116], D. Caffarri[35,92], H. Caines[141], A. Caliva[63,106], E. Calvo Villar[111], P. Camerini[25], A. A. Capon[113], F. Carena[35], W. Carena[35], F. Carnesecchi[12,27], J. Castillo Castellanos[75], A. J. Castro[127], E. A. R. Casula[54], C. Ceballos Sanchez[9], S. Chandra[137], B. Chang[125], W. Chang[7], S. Chapeland[35], M. Chartier[126], S. Chattopadhyay[137], S. Chattopadhyay[109], A. Chauvin[36,105], C. Cheshkov[132], B. Cheynis[132], V. Chibante Barroso[35], D. D. Chinellato[122], S. Cho[60], P. Chochula[35], M. Chojnacki[91], S. Choudhury[137], T. Chowdhury[131], P. Christakoglou[92], C. H. Christensen[91], P. Christiansen[34], T. Chujo[130], S. U. Chung[19], C. Cicalo[54], L. Cifarelli[12,27], F. Cindolo[53], J. Cleymans[100], F. Colamaria[33,52], D. Colella[35,52,65], A. Collu[82], M. Colocci[27], M. Concas[58,b], G. Conesa Balbastre[81], Z. Conesa del Valle[61], J. G. Contreras[39], T. M. Cormier[95], Y. Corrales Morales[58], I. Cortés Maldonado[2], P. Cortese[32], M. R. Cosentino[123], F. Costa[35], S. Costanza[134], J. Crkovská[61], P. Crochet[131], E. Cuautle[72], L. Cunqueiro[71,95], T. Dahms[36,105], A. Dainese[56], M. C. Danisch[104], A. Danu[68], D. Das[109], I. Das[109], S. Das[4], A. Dash[88], S. Dash[48], S. De[49], A. De Caro[30], G. de Cataldo[52], C. de Conti[121], J. de Cuveland[42], A. De Falco[24], D. De Gruttola[12,30], N. De Marco[58], S. De Pasquale[30], R. D. De Souza[122], H. F. Degenhardt[121], A. Deisting[104,106], A. Deloff[86], C. Deplano[92], P. Dhankher[48], D. Di Bari[33], A. Di Mauro[35], P. Di Nezza[51], B. Di Ruzza[56], M. A. Diaz Corchero[10], T. Dietel[100], P. Dillenseger[70], Y. Ding[7], R. Divià[35], Ø. Djuvsland[23], A. Dobrin[35], D. Domenicis Gimenez[121], B. Dönigus[70], O. Dordic[21], L. V. R. Doremalen[63], A. K. Dubey[137], A. Dubla[106], L. Ducroux[132], S. Dudi[99], A. K. Duggal[99], M. Dukhishyam[88], P. Dupieux[131], R. J. Ehlers[141],

D. Elia[52], E. Endress[111], H. Engel[69], E. Epple[141], B. Erazmus[114], F. Erhardt[98], B. Espagnon[61], G. Eulisse[35], J. Eum[19], D. Evans[110], S. Evdokimov[112], L. Fabbietti[36,105], J. Faivre[81], A. Fantoni[51], M. Fasel[95], L. Feldkamp[71], A. Feliciello[58], G. Feofilov[136], A. Fernández Téllez[2], E. G. Ferreiro[16], A. Ferretti[26], A. Festanti[29,35], V. J. G. Feuillard[75,131], J. Figiel[118], M. A. S. Figueredo[121], S. Filchagin[108], D. Finogeev[62], F. M. Fionda[22,24], M. Floris[35], S. Foertsch[76], P. Foka[106], S. Fokin[90], E. Fragiacomo[59], A. Francescon[35], A. Francisco[114], U. Frankenfeld[106], G. G. Fronze[26], U. Fuchs[35], C. Furget[81], A. Furs[62], M. Fusco Girard[30], J. J. Gaardhøje[91], M. Gagliardi[26], A. M. Gago[111], K. Gajdosova[91], M. Gallio[26], C. D. Galvan[120], P. Ganoti[85], C. Garabatos[106], E. Garcia-Solis[13], K. Garg[28], C. Gargiulo[35], P. Gasik[36,105], E. F. Gauger[119], M. B. Gay Ducati[73], M. Germain[114], J. Ghosh[109], P. Ghosh[137], S. K. Ghosh[4], P. Gianotti[51], P. Giubellino[35,58,106], P. Giubilato[29], E. Gladysz-Dziadus[118], P. Glässel[104], D. M. Gómez Coral[74], A. Gomez Ramirez[69], A. S. Gonzalez[35], V. Gonzalez[10], P. González-Zamora[10,2], S. Gorbunov[42], L. Görlich[118], S. Gotovac[117], V. Grabski[74], L. K. Graczykowski[138], K. L. Graham[110], L. Greiner[82], A. Grelli[63], C. Grigoras[35], V. Grigoriev[83], A. Grigoryan[1], S. Grigoryan[77], J. M. Gronefeld[106], F. Grosa[31], J. F. Grosse-Oetringhaus[35], R. Grosso[106], F. Guber[62], R. Guernane[81], B. Guerzoni[27], K. Gulbrandsen[91], T. Gunji[129], A. Gupta[101], R. Gupta[101], I. B. Guzman[2], R. Haake[35], C. Hadjidakis[61], H. Hamagaki[84], G. Hamar[140], J. C. Hamon[133], M. R. Haque[63], J. W. Harris[141], A. Harton[13], H. Hassan[81], D. Hatzifotiadou[12,53], S. Hayashi[129], S. T. Heckel[70], E. Hellbär[70], H. Helstrup[37], A. Herghelegiu[87], E. G. Hernandez[2], G. Herrera Corral[11], F. Herrmann[71], B. A. Hess[103], K. F. Hetland[37], H. Hillemanns[35], C. Hills[126], B. Hippolyte[133], B. Hohlweger[105], D. Horak[39], S. Hornung[106], R. Hosokawa[81,130], P. Hristov[35], C. Hughes[127], T. J. Humanic[18], N. Hussain[44], T. Hussain[17], D. Hutter[42], D. S. Hwang[20], S. A. Iga Buitron[72], R. Ilkaev[108], M. Inaba[130], M. Ippolitov[83,90], M. S. Islam[109], M. Ivanov[106], V. Ivanov[96], V. Izucheev[112], B. Jacak[82], N. Jacazio[27], P. M. Jacobs[82], M. B. Jadhav[48], S. Jadlovska[116], J. Jadlovsky[116], S. Jaelani[63], C. Jahnke[36], M. J. Jakubowska[138], M. A. Janik[138], P. H. S. Y. Jayarathna[124], C. Jena[88], M. Jercic[98], R. T. Jimenez Bustamante[106], P. G. Jones[110], A. Jusko[110], P. Kalinak[65], A. Kalweit[35], J. H. Kang[142], V. Kaplin[83], S. Kar[137], A. KarasuUysal[80], O. Karavichev[62], T. Karavicheva[62], L. Karayan[104,106], P. Karczmarczyk[35], E. Karpechev[62], U. Kebschull[69], R. Keidel[143], D. L. D. Keijdener[63], M. Keil[35], B. Ketzer[45], Z. Khabanova[92], P. Khan[109], S. A. Khan[137], A. Khanzadeev[96], Y. Kharlov[112], A. Khatun[17], A. Khuntia[49], M. M. Kielbowicz[118], B. Kileng[37], B. Kim[130], D. Kim[142], D. J. Kim[125], H. Kim[142], J. S. Kim[43], J. Kim[104], M. Kim[60], S. Kim[20], T. Kim[142], S. Kirsch[42], I. Kisel[42], S. Kiselev[64], A. Kisiel[138], G. Kiss[140], J. L. Klay[6], C. Klein[70], J. Klein[35], C. Klein-Bösing[71], S. Klewin[104], A. Kluge[35], M. L. Knichel[35,104], A. G. Knospe[124], C. Kobdaj[115], M. Kofarago[140], M. K. Köhler[104], T. Kollegger[106], V. Kondratiev[136], N. Kondratyeva[83], E. Kondratyuk[112], A. Konevskikh[62], M. Konyushikhin[139], M. Kopcik[116], M. Kour[101], C. Kouzinopoulos[35], O. Kovalenko[86], V. Kovalenko[136], M. Kowalski[118], G. Koyithatta Meethaleveedu[48], I. Králik[65], A. Kravčáková[40], L. Kreis[106], M. Krivda[65,110], F. Krizek[94], E. Kryshen[96], M. Krzewicki[42], A. M. Kubera[18], V. Kučera[94], C. Kuhn[133], P. G. Kuijer[92], A. Kumar[101], J. Kumar[48], L. Kumar[99], S. Kumar[48], S. Kundu[88], P. Kurashvili[86], A. Kurepin[62], A. B. Kurepin[62], A. Kuryakin[108], S. Kushpil[94], M. J. Kweon[60], Y. Kwon[142], S. L. La Pointe[42], P. La Rocca[28], C. Lagana Fernandes[121], Y. S. Lai[82], I. Lakomov[35], R. Langoy[141], K. Lapidus[141], C. Lara[69], A. Lardeux[21], A. Lattuca[26], E. Laudi[35], R. Lavicka[39], R. Lea[25], L. Leardini[104], S. Lee[142], F. Lehas[92], S. Lehner[113], J. Lehrbach[42], R. C. Lemmon[93], E. Leogrande[63], I. León Monzón[120], P. Lévai[140], X. Li[14], J. Lien[41], R. Lietava[110], B. Lim[19], S. Lindal[21], V. Lindenstruth[42], S. W. Lindsay[126], C. Lippmann[106], M. A. Lisa[18], V. Litichevskyi[46], W. J. Llope[139], D. F. Lodato[63], P. I. Loenne[22], V. Loginov[83], C. Loizides[82,95], P. Loncar[117], X. Lopez[131], E. López Torres[9], A. Lowe[140], P. Luettig[70], J. R. Luhder[71], M. Lunardon[29], G. Luparello[25,59], M. Lupi[35], T. H. Lutz[141], A. Maevskaya[62], M. Mager[35], S. M. Mahmood[21], A. Maire[133], R. D. Majka[141], M. Malaev[96], L. Malinina[77,iii], D. Mal'Kevich[64], P. Malzacher[106], A. Mamonov[108], V. Manko[90], F. Manso[131], V. Manzari[52], Y. Mao[7], M. Marchisone[76,128,132], J. Mareš[66], G. V. Margagliotti[25], A. Margotti[53], J. Margutti[63], A. Marín[106], C. Markert[119], M. Marquard[70], N. A. Martin[106], P. Martinengo[35], J. A. L. Martinez[69], M. I. Martínez[2], G. Martínez García[114], M. Martinez Pedreira[35], S. Masciocchi[106], M. Masera[26], A. Masoni[54], E. Masson[114], A. Mastroserio[52], A. M. Mathis[36,105], P. F. T. Matuoka[121], A. Matyja[127], C. Mayer[118], J. Mazer[127], M. Mazzilli[33], M. A. Mazzoni[57], F. Meddi[23], Y. Melikyan[83], A. Menchaca-Rocha[74], E. Meninno[30], J. Mercado Pérez[104], M. Meres[38], S. Mhlanga[100], Y. Miake[130], M. M. Mieskolainen[46], D. L. Mihaylov[105], K. Mikhaylov[64,77], A. Mischke[63], A. N. Mishra[49], D. Miśkowiec[106], J. Mitra[137], C. M. Mitu[68], N. Mohammadi[63], A. P. Mohanty[63], B. Mohanty[88], M. Mohisin Khan[17,d], E. Montes[10], D. A. Moreira De Godoy[71], L. A. P. Moreno[2], S. Moretto[29], A. Morreale[114], A. Morsch[35], V. Muccifora[51], E. Mudnic[117], D. Mühlheim[71], S. Muhuri[137], J. D. Mulligan[141], M. G. Munhoz[121], K. Münning[45], R. H. Munzer[70], H. Murakami[129], S. Murray[76], L. Musa[35], J. Musinsky[65], C. J. Myers[124], J. W. Myrcha[138], D. Nag[4], B. Naik[48], R. Nair[86], B. K. Nandi[48], R. Nania[12,53], E. Nappi[52], A. Narayan[48], M. U. Naru[15], H. Natal da Luz[121], C. Nattrass[127], S. R. Navarro[2], K. Nayak[88], R. Nayak[48], T. K. Nayak[137], S. Nazarenko[108], R. A. Negrao De Oliveira[35,70], L. Nellen[72], S. V. Nesbo[37], F. Ng[124], M. Nicassio[106], M. Niculescu[68], J. Niedziela[35,138], B. S. Nielsen[91], S. Nikolaev[90], S. Nikulin[90], V. Nikulin[96], F. Noferini[12,53], P. Nomokonov[77], G. Nooren[63], J. C. C. Noris[2], J. Norman[126], A. Nyanin[90], J. Nystrand[22],

H. Oeschler[19,104,i],   H. Oh[142],   A. Ohlson[104],   T. Okubo[47],   L. Olah[140],   J. Oleniacz[138],   A. C. Oliveira Da Silva[121], M. H. Oliver[141], J. Onderwaater[106], C. Oppedisano[58], R. Orava[46], M. Oravec[116], A. Ortiz Velasquez[72], A. Oskarsson[34], J. Otwinowski[118], K. Oyama[84], Y. Pachmayer[104], V. Pacik[91], D. Pagano[135], G. Paić[72], P. Palni[7], J. Pan[139], A. K. Pandey[48], S. Panebianco[75], V. Papikyan[1], P. Pareek[49], J. Park[60], S. Parmar[99], A. Passfeld[71], S. P. Pathak[124], R. N. Patra[137], B. Paul[58], H. Pei[7], T. Peitzmann[63], X. Peng[7], L. G. Pereira[73], H. Pereira Da Costa[75], D. Peresunko[83,90], E. Perez Lezama[70], V. Peskov[70], Y. Pestov[5], V. Petráček[39], V. Petrov[112], M. Petrovici[87], C. Petta[28], R. P. Pezzi[73], S. Piano[59], M. Pikna[38], P. Pillot[114], L. O. D. L. Pimentel[91], O. Pinazza[35,53], L. Pinsky[124], D. B. Piyarathna[124], M. Płoskoń[82], M. Planinic[98], F. Pliquett[70], J. Pluta[138], S. Pochybova[140], P. L. M. Podesta-Lerma[120], M. G. Poghosyan[95], B. Polichtchouk[112], N. Poljak[98], W. Poonsawat[115], A. Pop[87], H. Poppenborg[71], S. Porteboeuf-Houssais[131], V. Pozdniakov[77], S. K. Prasad[4], R. Preghenella[53], F. Prino[58], C. A. Pruneau[139], I. Pshenichnov[62], M. Puccio[26], V. Punin[108], J. Putschke[139], S. Raha[4], S. Rajput[101], J. Rak[125], A. Rakotozafindrabe[75], L. Ramello[32], F. Rami[133], D. B. Rana[124], R. Raniwala[102], S. Raniwala[102], S. S. Räsänen[46], B. T. Rascanu[70], D. Rathee[99], V. Ratza[45], I. Ravasenga[31], K. F. Read[95,127], K. Redlich[86,e], A. Rehman[22], P. Reichelt[70], F. Reidt[35], X. Ren[7], R. Renfordt[70], A. Reshetin[62], K. Reygers[104], V. Riabov[96], T. Richert[34,63], M. Richter[21], P. Riedler[35], W. Riegler[35], F. Riggi[28], C. Ristea[68], M. Rodríguez Cahuantzi[2], K. Røed[21], E. Rogochaya[77], D. Rohr[35,42], D. Röhrich[32], P. S. Rokita[138], F. Ronchetti[51], E. D. Rosas[72], P. Rosnet[131], A. Rossi[29,56], A. Rotondi[134], F. Roukoutakis[85], C. Roy[133], P. Roy[109], A. J. Rubio Montero[10], O. V. Rueda[72], R. Rui[25], B. Rumyantsev[77], A. Rustamov[89], E. Ryabinkin[90], Y. Ryabov[96], A. Rybicki[118], S. Saarinen[46], S. Sadhu[137], S. Sadovsky[112], K. Šafařík[35], S. K. Saha[137], B. Sahlmuller[70], B. Sahoo[48], P. Sahoo[49], R. Sahoo[49], S. Sahoo[67], P. K. Sahu[67], J. Saini[137], S. Sakai[130], M. A. Saleh[139], J. Salzwedel[18], S. Sambyal[101], V. Samsonov[83,96], A. Sandoval[74], A. Sarkar[76], D. Sarkar[137], N. Sarkar[137], P. Sarma[44], M. H. P. Sas[63], E. Scapparone[53], F. Scarlassara[29], B. Schaefer[95], H. S. Scheid[70], C. Schiaua[87], R. Schicker[104], C. Schmidt[106], H. R. Schmidt[103], M. O. Schmidt[104], M. Schmidt[103], N. V. Schmidt[70,95], J. Schukraft[35], Y. Schutz[35,133], K. Schwarz[106], K. Schweda[106], G. Scioli[27], E. Scomparin[58], M. Šefčík[40], J. E. Seger[97], Y. Sekiguchi[129], D. Sekihata[47], I. Selyuzhenkov[83,106], K. Senosi[76], S. Senyukov[133], E. Serradilla[74,10], P. Sett[48], A. Sevcenco[68], A. Shabanov[62], A. Shabetai[114], R. Shahoyan[35], W. Shaikh[109], A. Shangaraev[112], A. Sharma[99], A. Sharma[101], M. Sharma[101], M. Sharma[101], N. Sharma[99], A. I. Sheikh[137], K. Shigaki[47], S. Shirinkin[64], Q. Shou[7], K. Shtejer[9,26], Y. Sibiriak[90], S. Siddhanta[54], K. M. Sielewicz[35], T. Siemiarczuk[86], S. Silaeva[90], D. Silvermyr[34], G. Simatovic[92], G. Simonetti[35], R. Singaraju[137], R. Singh[88], V. Singhal[137], T. Sinha[109], B. Sitar[38], M. Sitta[32], T. B. Skaali[21], M. Slupecki[125], N. Smirnov[141], R. J. M. Snellings[63], T. W. Snellman[125], J. Song[19], M. Song[142], F. Soramel[29], S. Sorensen[127], F. Sozzi[106], I. Sputowska[118], J. Stachel[104], I. Stan[68], P. Stankus[95], E. Stenlund[34], D. Stocco[114], M. M. Storetvedt[37], P. Strmen[38], A. A. P. Suaide[121], T. Sugitate[47], C. Suire[61], M. Suleymanov[15], M. Suljic[25], R. Sultanov[64], M. Šumbera[94], S. Sumowidagdo[50], K. Suzuki[113], S. Swain[67], A. Szabo[38], I. Szarka[38], U. Tabassam[15], J. Takahashi[122], G. J. Tambave[22], N. Tanaka[130], M. Tarhini[61], M. Tariq[17], M. G. Tarzila[87], A. Tauro[35], G. Tejeda Muñoz[2], A. Telesca[35], K. Terasaki[129], C. Terrevoli[29], B. Teyssier[132], D. Thakur[49], S. Thakur[137], D. Thomas[119], F. Thoresen[91], R. Tieulent[132], A. Tikhonov[62], A. R. Timmins[124], A. Toia[70], M. Toppi[51], S. R. Torres[120], S. Tripathy[49], S. Trogolo[26], G. Trombetta[33], L. Tropp[40], V. Trubnikov[3], W. H. Trzaska[125], B. A. Trzeciak[63], T. Tsuji[129], A. Tumkin[108], R. Turrisi[56], T. S. Tveter[21], K. Ullaland[22], E. N. Umaka[124], A. Uras[132], G. L. Usai[24], A. Utrobicic[98], M. Vala[65,116], J. Van Der Maarel[63], J. W. Van Hoorne[35], M. van Leeuwen[63], T. Vanat[94], P. Vande Vyvre[35], D. Varga[140], A. Vargas[2], M. Vargyas[125], R. Varma[48], M. Vasileiou[85], A. Vasiliev[90], A. Vauthier[81], O. Vázquez Doce[36,105], V. Vechernin[136], A. M. Veen[63], A. Velure[22], E. Vercellin[26], S. Vergara Limón[2], R. Vernet[8], R. Vértesi[140], L. Vickovic[117], S. Vigolo[63], J. Viinikainen[125], Z. Vilakazi[128], O. Villalobos Baillie[110], A. Villatoro Tello[2], A. Vinogradov[90], L. Vinogradov[136], T. Virgili[30], V. Vislavicius[34], A. Vodopyanov[77], M. A. Völkl[103], K. Voloshin[64], S. A. Voloshin[139], G. Volpe[33], B. von Haller[35], I. Vorobyev[36,105], D. Voscek[116], D. Vranic[35,106], J. Vrláková[40], B. Wagner[22], H. Wang[63], M. Wang[7], D. Watanabe[130], Y. Watanabe[129,130], M. Weber[113], S. G. Weber[106], D. F. Weiser[104], S. C. Wenzel[35], J. P. Wessels[71], U. Westerhoff[71], A. M. Whitehead[100], J. Wiechula[70], J. Wikne[21], G. Wilk[86], J. Wilkinson[53,104], G. A. Willems[35,71], M. C. S. Williams[53], E. Willsher[110], B. Windelband[104], W. E. Witt[127], R. Xu[7], S. Yalcin[80], K. Yamakawa[47], P. Yang[7], S. Yano[47], Z. Yin[7], H. Yokoyama[81,130], I.-K. Yoo[19], J. H. Yoon[60], E. Yun[19], V. Yurchenko[3], V. Zaccolo[58], A. Zaman[15], C. Zampolli[35], H. J. C. Zanoli[121], N. Zardoshti[110], A. Zarochentsev[136], P. Závada[66], N. Zaviyalov[108], H. Zbroszczyk[138], M. Zhalov[96], H. Zhang[7,22], X. Zhang[7], Y. Zhang[7], C. Zhang[63], Z. Zhang[7,131], C. Zhao[21], N. Zhigareva[64], D. Zhou[7], Y. Zhou[91], Z. Zhou[22], H. Zhu[22], J. Zhu[7], Y. Zhu[7], A. Zichichi[12,27], M. B. Zimmermann[35], G. Zinovjev[3], J. Zmeskal[113], S. Zou[7]

[1] A.I. Alikhanyan National Science Laboratory (Yerevan Physics Institute) Foundation, Yerevan, Armenia

[2] Benemérita Universidad Autónoma de Puebla, Puebla, Mexico

[3] Bogolyubov Institute for Theoretical Physics, Kiev, Ukraine

[4] Bose Institute, Department of Physics and Centre for Astroparticle Physics and Space Science (CAPSS), Kolkata, India

[5] Budker Institute for Nuclear Physics, Novosibirsk, Russia

[6] California Polytechnic State University, San Luis Obispo, CA, USA

[7] Central China Normal University, Wuhan, China

[8] Centre de Calcul de l'IN2P3, Villeurbanne, Lyon, France

[9] Centro de Aplicaciones Tecnológicas y Desarrollo Nuclear (CEADEN), Havana, Cuba

[10] Centro de Investigaciones Energéticas Medioambientales y Tecnológicas (CIEMAT), Madrid, Spain

[11] Centro de Investigación y de Estudios Avanzados (CINVESTAV), Mexico City and Mérida, Mexico

[12] Centro Fermi-Museo Storico della Fisica e Centro Studi e Ricerche "Enrico Fermi", Rome, Italy

[13] Chicago State University, Chicago, IL, USA

[14] China Institute of Atomic Energy, Beijing, China

[15] COMSATS Institute of Information Technology (CIIT), Islamabad, Pakistan

[16] Departamento de Física de Partículas and IGFAE, Universidad de Santiago de Compostela, Santiago de Compostela, , Spain

[17] Department of Physics, Aligarh Muslim University, Aligarh, India

[18] Department of Physics, Ohio State University, Columbus, OH, USA

[19] Department of Physics, Pusan National University, Pusan, Republic of Korea

[20] Department of Physics, Sejong University, Seoul, Republic of Korea

[21] Department of Physics, University of Oslo, Oslo, Norway

[22] Department of Physics and Technology, University of Bergen, Bergen, Norway

[23] Dipartimento di Fisica dell'Università 'La Sapienza' and Sezione INFN, Rome, Italy

[24] Dipartimento di Fisica dell'Università and Sezione INFN, Cagliari, Italy

[25] Dipartimento di Fisica dell'Università and Sezione INFN, Trieste, Italy

[26] Dipartimento di Fisica dell'Università and Sezione INFN, Turin, Italy

[27] Dipartimento di Fisica e Astronomia dell'Università and Sezione INFN, Bologna, Italy

[28] Dipartimento di Fisica e Astronomia dell'Università and Sezione INFN, Catania, Italy

[29] Dipartimento di Fisica e Astronomia dell'Università and Sezione INFN, Padova, Italy

[30] Dipartimento di Fisica 'E.R. Caianiello' dell'Università and Gruppo Collegato INFN, Salerno, Italy

[31] Dipartimento DISAT del Politecnico and Sezione INFN, Turin, Italy

[32] Dipartimento di Scienze e Innovazione Tecnologica dell'Università del Piemonte Orientale and INFN Sezione di Torino, Alessandria, Italy

[33] Dipartimento Interateneo di Fisica 'M. Merlin' and Sezione INFN, Bari, Italy

[34] Division of Experimental High Energy Physics, University of Lund, Lund, Sweden

[35] European Organization for Nuclear Research (CERN), Geneva, Switzerland

[36] Excellence Cluster Universe, Technische Universität München, Munich, Germany

[37] Faculty of Engineering, Bergen University College, Bergen, Norway

[38] Faculty of Mathematics, Physics and Informatics, Comenius University, Bratislava, Slovakia

[39] Faculty of Nuclear Sciences and Physical Engineering, Czech Technical University in Prague, Prague, Czech Republic

[40] Faculty of Science, P.J. Šafárik University, Košice, Slovakia

[41] Faculty of Technology, Buskerud and Vestfold University College, Tonsberg, Norway

[42] Frankfurt Institute for Advanced Studies, Johann Wolfgang Goethe-Universität Frankfurt, Frankfurt, Germany

[43] Gangneung-Wonju National University, Gangneung, Republic of Korea

[44] Department of Physics, Gauhati University, Guwahati, India

[45] Helmholtz-Institut für Strahlen- und Kernphysik, Rheinische Friedrich-Wilhelms-Universität Bonn, Bonn, Germany

[46] Helsinki Institute of Physics (HIP), Helsinki, Finland

[47] Hiroshima University, Hiroshima, Japan

[48] Indian Institute of Technology Bombay (IIT), Mumbai, India

[49] Indian Institute of Technology Indore, Indore, India

[50] Indonesian Institute of Sciences, Jakarta, Indonesia

[51] INFN, Laboratori Nazionali di Frascati, Frascati, Italy

[52] INFN, Sezione di Bari, Bari, Italy

[53] INFN, Sezione di Bologna, Bologna, Italy

[54] INFN, Sezione di Cagliari, Cagliari, Italy

[55] INFN, Sezione di Catania, Catania, Italy

[56] INFN, Sezione di Padova, Padova, Italy

[57] INFN, Sezione di Roma, Rome, Italy

[58] INFN, Sezione di Torino, Turin, Italy

[59] INFN, Sezione di Trieste, Trieste, Italy

[60] Inha University, Incheon, Republic of Korea

[61] Institut de Physique Nucléaire d'Orsay (IPNO), Université Paris-Sud, CNRS-IN2P3, Orsay, France

[62] Institute for Nuclear Research, Academy of Sciences, Moscow, Russia

[63] Institute for Subatomic Physics of Utrecht University, Utrecht, Netherlands

[64] Institute for Theoretical and Experimental Physics, Moscow, Russia

[65] Institute of Experimental Physics, Slovak Academy of Sciences, Košice, Slovakia

[66] Institute of Physics, Academy of Sciences of the Czech Republic, Prague, Czech Republic

[67] Institute of Physics, Bhubaneswar, India

[68] Institute of Space Science (ISS), Bucharest, Romania

[69] Institut für Kernphysik, Johann Wolfgang Goethe-Universität Frankfurt, Frankfurt, Germany

[70] Institut für Kernphysik, Johann Wolfgang Goethe-Universität Frankfurt, Frankfurt, Germany

[71] Institut für Kernphysik, Westfälische Wilhelms-Universität Münster, Münster, Germany

[72] Instituto de Ciencias Nucleares, Universidad Nacional Autónoma de México, Mexico City, Mexico

[73] Instituto de Física, Universidade Federal do Rio Grande do Sul (UFRGS), Porto Alegre, Brazil

[74] Instituto de Física, Universidad Nacional Autónoma de México, Mexico City, Mexico

[75] IRFU, CEA, Université Paris-Saclay, Saclay, France

[76] iThemba LABS, National Research Foundation, Somerset West, South Africa

[77] Joint Institute for Nuclear Research (JINR), Dubna, Russia

[78] Konkuk University, Seoul, Republic of Korea

[79] Korea Institute of Science and Technology Information, Daejeon, Republic of Korea

[80] KTO Karatay University, Konya, Turkey

[81] Laboratoire de Physique Subatomique et de Cosmologie, Université Grenoble-Alpes, CNRS-IN2P3, Grenoble, France

[82] Lawrence Berkeley National Laboratory, Berkeley, CA, USA

[83] Moscow Engineering Physics Institute, Moscow, Russia

[84] Nagasaki Institute of Applied Science, Nagasaki, Japan

[85] Physics Department, National and Kapodistrian University of Athens, Athens, Greece

[86] National Centre for Nuclear Studies, Warsaw, Poland

[87] National Institute for Physics and Nuclear Engineering, Bucharest, Romania

[88] National Institute of Science Education and Research, HBNI, Jatni, India

[89] National Nuclear Research Center, Baku, Azerbaijan

[90] National Research Centre Kurchatov Institute, Moscow, Russia

[91] Niels Bohr Institute, University of Copenhagen, Copenhagen, Denmark

[92] Nikhef, Nationaal instituut voor subatomaire fysica, Amsterdam, Netherlands

[93] Nuclear Physics Group, STFC Daresbury Laboratory, Daresbury, United Kingdom

[94] Nuclear Physics Institute, Academy of Sciences of the Czech Republic, Řež u Prahy, , Czech Republic

[95] Oak Ridge National Laboratory, Oak Ridge, TN, USA

[96] Petersburg Nuclear Physics Institute, Gatchina, Russia

[97] Physics Department, Creighton University, Omaha, NE, Tennessee

[98] Physics Department, Faculty of science, University of Zagreb, Zagreb, Croatia

[99] Physics Department, Panjab University, Chandigarh, India

[100] Physics Department, University of Cape Town, Cape Town, South Africa

[101] Physics Department, University of Jammu, Jammu, India

[102] Physics Department, University of Rajasthan, Jaipur, India

[103] Physikalisches Institut, Eberhard-Karls-Universität Tübingen, Tübingen, Germany

[104] Physikalisches Institut, Ruprecht-Karls-Universität Heidelberg, Heidelberg, Germany

[105] Physik Department, Technische Universität München, Munich, Germany

[106] Research Division and ExtreMe Matter Institute EMMI, GSI Helmholtzzentrum für Schwerionenforschung GmbH, Darmstadt, Germany

[107] Rudjer Bošković Institute, Zagreb, Croatia

[108] Russian Federal Nuclear Center (VNIIEF), Sarov, Russia

[109] Saha Institute of Nuclear Physics, Kolkata, India

[110] School of Physics and Astronomy, University of Birmingham, Birmingham, United Kingdom

[111] Sección Física, Departamento de Ciencias, Pontificia Universidad Católica del Perú, Lima, Peru

[112] SSC IHEP of NRC Kurchatov institute, Protvino, Russia

[113] Stefan Meyer Institut für Subatomare Physik (SMI), Vienna, Austria

[114] SUBATECH, IMT Atlantique, Université de Nantes, CNRS-IN2P3, Nantes, France

[115] Suranaree University of Technology, Nakhon Ratchasima, Thailand

[116] Technical University of Košice, Košice, Slovakia

[117] Technical University of Split FESB, Split, Croatia

[118] The Henryk Niewodniczanski Institute of Nuclear Physics, Polish Academy of Sciences, Cracow, Poland

[119] Physics Department, The University of Texas at Austin, Austin, TX, USA

[120] Universidad Autónoma de Sinaloa, Culiacán, Mexico

[121] Universidade de São Paulo (USP), São Paulo, Brazil

[122] Universidade Estadual de Campinas (UNICAMP), Campinas, Brazil

[123] Universidade Federal do ABC, Santo Andre, Brazil

[124] University of Houston, Houston, TX, USA

[125] University of Jyväskylä, Jyväskylä, Finland

[126] University of Liverpool, Liverpool, United Kingdom

[127] University of Tennessee, Knoxville, TN, USA

[128] University of the Witwatersrand, Johannesburg, South Africa

[129] University of Tokyo, Tokyo, Japan

[130] University of Tsukuba, Tsukuba, Japan

[131] Université Clermont Auvergne, CNRS/IN2P3, LPC, Clermont-Ferrand, France

[132] Université de Lyon, Université Lyon 1, CNRS/IN2P3, IPN-Lyon, Villeurbanne, Lyon, France

[133] Université de Strasbourg, CNRS, IPHC UMR 7178, Strasbourg, France

[134] Università degli Studi di Pavia, Pavia, Italy

[135] Università di Brescia, Brescia, Italy

[136] V. Fock Institute for Physics, St. Petersburg State University, St. Petersburg, Russia

[137] Variable Energy Cyclotron Centre, Kolkata, India

[138] Warsaw University of Technology, Warsaw, Poland

[139] Wayne State University, Detroit, MI, USA

[140] Wigner Research Centre for Physics, Hungarian Academy of Sciences, Budapest, Hungary

[141] Yale University, New Haven, CT, USA

[142] Yonsei University, Seoul, Republic of Korea

[143] Zentrum für Technologietransfer und Telekommunikation (ZTT), Fachhochschule Worms, Worms, Germany

[a] Deceased

[b] Dipartimento DET del Politecnico di Torino, Turin, Italy

[c] M.V. Lomonosov Moscow State University, D.V. Skobeltsyn Institute of Nuclear, Physics, Moscow, Russia

[d] Department of Applied Physics, Aligarh Muslim University, Aligarh, India

[e] Institute of Theoretical Physics, University of Wroclaw, Poland